



**IMPROVED DIRECT TORQUE CONTROL IN DUAL INVERTERS
USING FLEXIBLE SECTOR DETECTOR AND DUTY CYCLE
TECHNIQUES**



DOCTOR OF PHILOSOPHY

2024



Faculty of Electrical Technology and Engineering

**IMPROVED DIRECT TORQUE CONTROL IN DUAL INVERTERS
USING FLEXIBLE SECTOR DETECTOR AND DUTY CYCLE
TECHNIQUES**

Muhammad Zaid bin Aihsan

اونيورسيتي تيكنيكل مليسيا ملاك
UNIVERSITI TEKNIKAL MALAYSIA MELAKA

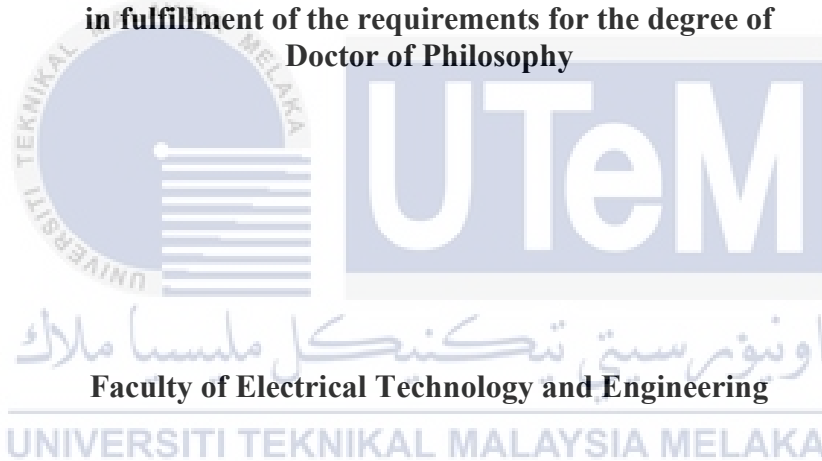
Doctor of Philosophy

2024

**IMPROVED DIRECT TORQUE CONTROL IN DUAL INVERTERS USING
FLEXIBLE SECTOR DETECTOR AND DUTY CYCLE TECHNIQUES**

MUHAMMAD ZAID BIN AIHSAN

**A thesis submitted
in fulfillment of the requirements for the degree of
Doctor of Philosophy**



UNIVERSITI TEKNIKAL MALAYSIA MELAKA

2024

DEDICATION

Special Dedication to:

My Respected Supervisor and Co-Supervisor,

Dr. Auzani bin Jidin and Dr. Azrita binti Alias

Thank you for your vital support, motivation, guidance, and supervision in accomplishing
this research.

My Beloved Parents,

Aihsan bin Adam and Rosnah binti Mohd

For supporting and encouraging me to complete this research

Thank you for your firm and gentle soul, which makes me who I am today.

My Lovely Wife,

Farah Wahida binti Bahador

For unwavering support and encouragement throughout this journey

Thank you for your love, patience, and understanding.

May God bless and protect them with happiness.

ABSTRACT

Direct Torque Control of Open-End Winding Induction Motor (DTC-OEWIM) is one of the techniques in motor drive applications that provides a robust and straightforward structure with excellent dynamic torque control. It controls the induction motor at both ends by using the dual-inverter circuit. Despite its outstanding performance, the DTC-OEWIM technique has several drawbacks. When the dual-inverter circuit is supplied with mismatched DC voltages, the direction of the medium voltage vectors will deviate and no longer tangential to the circular flux locus. This will cause significant stator flux droop and distortion in the stator currents, leading to poor torque regulation. Even though the DTC-OEWIM technique is famous for reducing torque ripples by using short voltage vectors, it is still unable to minimize them, especially during low-speed operations entirely. A flexible sector detector proposes to overcome the problems by generating a new sector that ensures the deviated voltage vectors are tangential to the circular flux locus. The study explored the potential of the proposed technique under steady-state and transient-state operation. Another objective was to design the duty cycle control technique to limit the surge torque slope during low-speed operation. Integrating duty cycle ratios into the default inverter switching restricts the torque increment and torque decrement rate. The proposed techniques were compared with the default DTC-OEWIM system and verified through simulation and experimental work. For simulation, MATLAB/Simulink software was used to design the complete system, using the exact parameters as in the hardware experimental setup. For experimental works, the setup consists of a dSPACE DS1104 controller, two units of a two-level inverter connected in a dual-inverter configuration, and a 1.1kW induction motor with a 2kW DC generator as a load. The results show a significant improvement: 1) the minimization of stator flux droop and distortion in stator currents, which in turn improves the torque regulation and 2) the reduction of torque ripples by up to 50% and the improvement in switching frequency during low-speed operation. In conclusion, the proposed technique effectively improves DTC-OEWIM while maintaining the simple structure of the DTC system.

**PENINGKATAN KAWALAN DAYAKILAS LANSUNG DALAM DWI
PENYONGSANG MENGGUNAKAN PENGESANAN SEKTOR BOLEH LENTUR
DAN TEKNIK KITAR TUGAS**

ABSTRAK

Kawalan Dayakilas Lansung daripada Motor Aruhan Belitan Tamatan Terbuka (DTC-OEWIM) adalah salah satu teknik dalam aplikasi pemacu motor yang menyediakan struktur yang teguh dan ringkas dengan kawalan dayakilas dinamik yang sangat baik. Ia mengawal motor aruhan pada kedua-dua tamatan dengan menggunakan litar dwi-penyongsang. Walaupun prestasinya yang cemerlang, teknik DTC-OEWIM mempunyai beberapa kelemahan. Apabila litar dwi-penyongsang dibekalkan dengan voltan DC yang tidak sepadan, arah vektor voltan sederhana akan terpesong dan tidak lagi bertanggen dengan bulatan lokus fluks. Sistem ini mengalami lelaian fluks pemegun yang besar dan juga gangguan pada arus pemegun yang membawa kepada pengaturan kilas yang lemah. Walaupun teknik DTC-OEWIM terkenal kerana keupayaannya untuk mengurangkan riak dayakilas dengan menggunakan vektor voltan pendek, ia masih tidak dapat meminimumkan sepenuhnya terutamanya semasa operasi berkelajuan rendah. Oleh itu, sebuah pengesan sektor yang boleh lentur dicadangkan untuk mengatasi masalah tersebut dengan menghasilkan sektor baru yang memastikan vektor voltan yang tersisih bersentuhan dengan bulatan lokus fluks. Kajian ini meneroka potensi teknik yang dicadangkan dalam operasi keadaan mantap dan keadaan berubah. Satu objektif lain ialah untuk merekabentuk teknik kawalan kitar tugas bagi menghadkan kemuncak cerun dayakilas ketika operasi kelajuan rendah. Ia dilakukan dengan mensepadakan nisbah kitar tugas ke dalam pensuisan penyongsang yang asal untuk menghadkan kadar peningkatan dan penurunan dayakilas. Teknik-teknik yang dicadangkan telah dibandingkan dengan sistem DTC-OEWIM yang asal dan disahkan melalui kerja simulasi dan eksperimen. Bagi simulasi, perisian MATLAB/Simulink digunakan bagi merekabentuk sistem yang lengkap dengan menggunakan parameter yang sama seperti dalam penyediaan eksperimen. Bagi kerja eksperimen, penyediaan penuh terdiri daripada pengawal dSPACE 1104, dua unit penyongsang dua aras yang disambungkan dalam tertatarajah dwi-penyongsang dan motor aruhan 1.1kW dengan penjana DC 2kW sebagai beban. Hasil kajian menunjukkan peningkatan yang bererti; 1) pengurangan lelai fluks pemegun dan gangguan pada arus pemegun, yang seterusnya meningkatkan kawalan dayakilas; dan 2) pengurangan riak dayakilas sehingga 50% dan penambahbaikan didalam frekuensi pensuisan dan sekali lagi semasa operasi kelajuan rendah. Kesimpulannya, teknik yang dicadangkan berkesan dalam menambah baik struktur DTC-OEWIM sambil mengekalkan stuktur mudah sistem DTC.

ACKNOWLEDGEMENT

In the name of Allah, the Most Gracious and the Most Merciful. Alhamdulillah, I praise and thank to Allah S.W.T for His boundless blessings and for granting me the strength and courage to successfully complete this thesis, titled "Improved Direct Torque Control in Dual Inverters using Flexible Sector Detector and Duty Cycle Techniques."

I want to express my deep gratitude to Universiti Teknikal Malaysia Melaka (UTeM) for providing me with excellent research facilities and an excellent environment. Furthermore, I sincerely thank my main supervisor, Dr. Auzani bin Jidin, and my co-supervisor, Dr. Azrita binti Alias, for their support, guidance, and knowledge. Their mentorship significantly contributed to the smooth progression of my PhD journey.

I sincerely thank my laboratory colleagues for the invaluable insights and knowledge-sharing throughout this research journey. Additionally, I am grateful to the members of Power Electronic and Drives (PEDS) research members and all those who provided physical and emotional support during the time.

Lastly, I want to thank my parents, wife, and siblings for their dua and for always being there for me, cheering me on, and never letting me give up on finishing my PhD. Their confidence in me has been a big motivation for my success.

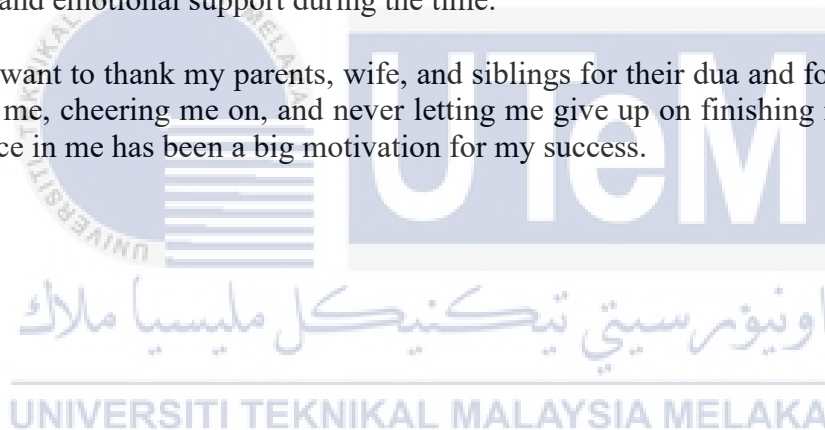


TABLE OF CONTENTS

	PAGES
DECLARATION	
APPROVAL	
DEDICATION	
ABSTRACT	i
ABSTRAK	ii
ACKNOWLEDGEMENT	iii
TABLE OF CONTENTS	v
LIST OF TABLES	ix
LIST OF FIGURES	x
LIST OF APPENDICES	xxi
LIST OF ABBREVIATIONS	xxii
LIST OF SYMBOLS	xxiv
LIST OF PUBLICATIONS	xxvi

CHAPTER

1. INTRODUCTION	1
1.1 Research Background	1
1.2 Problem Statement	4
1.3 Research Question	5
1.4 Research Objective	5
1.5 Research Scopes	6
1.6 Research Limitations	7
1.7 Research Flow Outlines	8
1.8 Thesis Outlines	10
2. LITERATURE REVIEW	12
2.1 Introduction	12
2.2 Field Oriented Control	13
2.2.1 Principle of Field Oriented Control	14
2.3 Direct Torque Control	17
2.3.1 Principle of Direct Torque Control	24
2.4 Estimation model	31
2.5 Stator flux droop and Sector definitions	33
2.6 Torque Ripples	35
2.7 Stator currents	36
2.8 Total Harmonic Distortion	37
2.9 The Evolution of Direct Torque Control and Associated Challenges	38
2.9.1 Direct Torque Control Open-End Winding Induction Motor (DTC-OEWIM)	40
2.9.1.1 DTC system with a sector rotation strategy	40
2.9.1.2 DTC system with duty cycle strategy	41

2.9.2	Direct Torque Control Open-End Winding Induction Motor (DTC-OEWIM)	42
2.9.2.1	DTC system using Virtual Voltage Space Vector	43
2.9.2.2	DTC system with Predictive torque control	45
2.9.2.3	DTC system with Common mode voltage minimization	48
2.9.2.4	DTC system with Fuzzy Logic Controller	50
2.9.2.5	DTC system using Carrier switching frequency	52
2.9.2.6	DTC system using Space Vector Modulation technique	54
2.9.2.7	DTC system using Bio-inspired algorithms	55
2.10	Literature Study and Identification of Research Gaps	59
2.11	Conclusion	62
3.	METHODOLOGY	64
3.1	Introduction	64
3.2	Research implementation flowchart	65
3.3	Mathematical model	68
3.4	Dual-Inverter technique using Open-End Winding Induction Motor	72
3.4.1	Dual-Inverter Switching Formulation	73
3.4.2	Flux Sectors definitions of default DTC-OEWIM system	81
3.5	Investigation of the mismatched supply voltage of dual-inverter	83
3.5.1	The effect of different voltage ratios on both inverters	84
3.6	DTC development by using flexible sector detector	89
3.6.1	Effects on resultant voltage vectors	89
3.6.2	Formulating proposed sector detector	90
3.6.3	Implementing new sector detector	93
3.7	Investigation of torque performance during low-speed operation	95
3.7.1	Comparison between DTC-SVV with DTC-LVV technique	97
3.8	DTC development by using duty cycle control technique for dual-inverter	99
3.8.1	DTC development using DCC1 scheme	100
3.8.2	DTC development using DCC2 scheme	103
3.9	Simulation setup	109
3.10	Conclusion	115
4.	RESULT AND DISCUSSION	117
4.1	Introduction	117
4.2	Steady-state operation of DTC OEWIM under matched DC voltage	118
4.2.1	Analysis of stator flux droop, φ_s and stator currents, i_s	118
4.2.2	Analysis of stator flux sector, d- and q- axis components of stator flux, φ_s and stator currents, i_s	122
4.2.3	Analysis of stator currents and stator flux locus	124
4.3	Steady- state operation of DTC OEWIM under mismatched DC voltage, $V_{dc1} = 100$ V, $V_{dc2} = 70$ V	126
4.3.1	Analysis of stator flux droop, φ_s and stator currents, i_s	126

4.3.2	Analysis of stator flux sector, d- and q- axis components of stator flux, φ_s and stator currents, i_s	130
4.3.3	Analysis of stator currents and stator flux locus	132
4.4	Steady- state operation of DTC OEWM under mismatched DC voltage, $V_{dc1} = 100 \text{ V}, V_{dc2} = 50 \text{ V}$	136
4.4.1	Analysis of stator flux droop, φ_s and stator currents, i_s	136
4.4.2	Analysis of stator flux sector, d- and q- axis components of stator flux, φ_s and stator currents, i_s	139
4.4.3	Analysis of stator currents and stator flux locus	142
4.5	Analysis of total harmonic distortion for matched and mismatched DC voltage	146
4.6	Analysis of Torque Dynamic and Speed Control Performances during Transient-State Operating Conditions	151
4.6.1	Analysis of Torque dynamic and Speed Control Performances for mismatched DC voltages ratio (100:100)	151
4.6.2	Analysis of Torque dynamic and Speed Control Performances for mismatched DC voltages ratio (100:70)	153
4.6.3	Analysis of Torque dynamic and Speed Control Performances for mismatched DC voltages ratio (100:50)	156
4.7	Minimization of torque ripple during low-speed operation	159
4.7.1	Analysis of torque ripple using DTC-LVV and DTC-SVV	160
4.7.2	Analysis of torque ripple using DTC-DCC1 technique	162
4.7.3	Analysis of torque ripple using DTC-DCC2 technique	164
4.7.4	Analysis of torque ripple using DTC-DCC2 technique with different hysteresis band size	165
4.8	Analysis of switching frequency	168
4.8.1	Analysis of switching frequency using DTC-LVV	168
4.8.2	Analysis of switching frequency using DTC-SVV	170
4.8.3	Analysis of switching frequency using DTC-DCC1	172
4.8.4	Analysis of switching frequency using DTC-DCC2	173
4.9	Analysis on Total Harmonic Distortion	175
4.10	Analysis of on dynamic operation of torque during low-speed operation	176
4.10.1	Analysis of of dynamic operation when using DTC-LVV	176
4.10.2	Analysis of of dynamic operation when using DTC-SVV	178
4.10.3	Analysis of of dynamic operation when using DTC-DCC1	180
4.10.4	Analysis of of dynamic operation when using DTC-DCC2	182
4.11	Summary	184

5. CONCLUSION AND RECOMMENDATIONS FOR FUTURE RESEARCH	186
5.1 Conclusions	186
5.2 Research Contributions	187
5.3 Suggestions for Future Works	188
REFERENCES	190
APPENDICES	209



LIST OF TABLES

TABLE	TITLE	PAGE
2.1	Look-up Table for Selecting Voltage Vectors	24
2.2	Optimized look-up Table under Predictive Torque Control (Venu et al., 2021)	47
2.3	Summary of Literature Review	60
3.1	Look-up Table for Switching Vectors in Dual Inverter	80
3.2	Magnitude voltage and angle direction for long voltage vectors	85
3.3	Magnitude voltage and angle direction for medium voltage vectors	85
3.4	Magnitude voltage and angle direction for short voltage vectors	86
3.5	MATLAB Simulink parameters	110
4.1	Performance of THD in overall cases including simulation and experimental conditions	150
4.2	Performance of THD in every DTC technique for both simulation and experimental results	175

LIST OF FIGURES

FIGURE	TITLE	PAGE
1.1	Vector control structure schemes (a) Field Oriented Control and (b) Direct Torque Control	2
1.2	Dual Inverters for Open-End Winding Induction Machine Drive	3
2.1	Closed loop constant V/f variable speed drive (Mikhael et al., 2016)	12
2.2	Indirect Field Oriented Control (Garcia et al., 1994)	14
2.3	Direct Field Oriented Control (Garcia et al., 1994)	15
2.4	Rotor Flux Vector is Aligned to d^e -axis	15
2.5	Conventional DTC system proposed by Takahashi and Noguchi (1986)	17
2.6	Three-Phase Voltage Source Inverter (a) Schematic circuit (b) Simplified circuit based on switching information	20
2.7	Voltage space vectors with the corresponded switching states	21
2.8	Control of Stator Flux (a) Two-Level hysteresis comparator (b) Typical Waveforms	25
2.9	Control of Stator Flux (a) Rotational Movement each sector (b) Default sector definition	27
2.10	Control of Torque (a) Three-Level hysteresis comparator (b) Typical Waveforms for controlling positive and negative torque slope	29
2.11	The selection of the optimum inverter output voltage vectors for every sector (Jidin et al., 2011)	30
2.12	Stator flux motions and rotor flux vectors	30
2.13	Flux estimation based on voltage model (Bose, 2002)	32
2.14	Flux estimation based on current model (Bose, 2002)	33
2.15	Stator flux magnitude with droop conditions on each sector	34

2.16	The switches of voltage vector at the boundary of sector in the conventional DTC by Takahashi and Noguchi (1986)	35
2.17	Visualization of torque ripple and torque error condition	36
2.18	Effects of selecting different switching under dynamic conditions (a) Stator voltage vector (b) Comparison of the load angle (Jidin et al., 2011)	40
2.19	The shifted sector by using fixed sector rotation strategy (Wong and Holliday, 2004)	41
2.20	Block diagram of the proposed MPTC DTC (Wong and Holliday, 2004)	42
2.21	(a) Virtual Space Vector diagram (b) Realization of space vector ' v_a ' (Suresh and Rajeevan, 2020)	44
2.22	(a) Virtual space vector for Inverter 1 and Inverter 2 (b) Realization of three-level space vector structure (Suresh and Rajeevan, 2018)	45
2.23	Block diagram of proposed predictive control (Venu et al., 2021)	47
2.24	Dual-Inverter technique using a single DC voltage source (Nirsha and Rajeevan, 2017)	48
2.25	Voltage space vector diagram of the proposed DTC scheme (Nirsha and Rajeevan, 2017)	49
2.26	(a) Traditional single-carrier PWM (b) Proposed Multicarrier PWM for three-phase two-level dual inverter drive system (Alcaide et al., 2021)	50
2.27	(a) Fuzzy logic controller for CHB-DTC (b) Membership function of fuzzy logic controller (Mortezaei et al., 2011)	51
2.28	Proposed fuzzy logic control integrated with dual inverter technique (El Ouanjli et al., 2019)	52
2.29	(a) Proposed torque controller (b) Typical waveform of the torque controller by Idris and Yatim (2004)	53
2.30	DTC-OEWIM technique using carrier-based torque controller (Rahim et al., 2016)	54
2.31	The proposed DTC-SVM induction machine (Lascu et al., 2000)	55

2.32	The pheromone placed by the ants for tracking purposes (Mahfoud et al., 2022)	56
2.33	The completed ACO-DTC control structure (Mahfoud et al., 2022)	57
2.34	Tuning process between the ACO technique and PID controller (Mahfoud et al., 2022)	58
2.35	Tuning process between the PSO technique and PID controller (Elgbaily et al., 2022)	59
2.36	A tree-diagram of research gaps and direction	61
3.1	Research Flowchart	66
3.2	Cross-Section of a Symmetrical Two-Pole Three-Phase Induction Machine	69
3.3	A block diagram of Mathematical Modeling of an Induction Machine	72
3.4	The configuration of dual-inverter technique	73
3.5	Stator Voltage in Space Vector form in d^s - and q^s -Axis plane	76
3.6	Space Voltage Vectors switching state for Dual-Inverter technique	79
3.7	Flux Sector for (a) Long and Short vectors (b) Medium vectors	82
3.8	The default dual-inverter technique for Open-End Winding DTC System	83
3.9	Comparison between matched and mismatched DC voltage in (a) Short vectors (b) Medium vectors and (c) Long vectors	86
3.10	Comparison of medium voltage vectors performance in (a) matched DC voltage (b) mismatched DC voltage	87
3.11	Comparison of medium voltage vectors performance in boundary default sector for (a) matched supply voltage (b) mismatched supply voltage	88
3.12	Generation of resultant voltage vectors (a) matched DC voltage (b) mismatched DC voltage	90

3.13	Remapping of new sectors for an inverter ratio of 100:50 (a) Partially for 3 voltage vectors (b) Complete 6 voltage vectors	91
3.14	Proposed modified sector block diagram in the DTC-OEWIM	92
3.15	Flowchart to determine the central angle for each sector for 100:50 ratio	93
3.16	New sector for mismatched DC voltage of inverter ratios of (a) 100:50 and (b) 100:70	94
3.17	The complete process of determining the proposed flexible sector detector	95
3.18	Typical torque slope pattern for low-speed and high-speed operation	96
3.19	Comparison of torque when using vectors from DTC-LVV and DTC-SVV	97
3.20	The variation of torque response and its torque error status when using DTC-LVV and DTC-SVV	98
3.21	The variation of torque response and its torque error status when using DTC-SVV and DTC-DCC1	101
3.22	A basic PWM controller adapt in the DTC-OEWIM as DTC-DCC1	102
3.23	The proposed structure of DTC-DCC1	103
3.24	An enhance PWM controller adapt in DTC-DCC2 technique	104
3.25	An enhance PWM controller in DTC-DCC2 technique	105
3.26	The complete PWM running in DTC-DCC2 technique	106
3.27	The variation of torque response and its torque error status when using DTC-SVV and DTC-DCC2 technique	107
3.28	The proposed structure of DTC-DCC2	108
3.29	The complete process of determining the DTC-DCC2	108
3.30	The default configuration of DTC using the dual inverter technique	109
3.31	The steady-state operation for the dual-inverter technique under mismatched voltage	111

3.32	The transient-state operation for the dual-inverter technique under mismatched voltage	112
3.33	The DTC system using DTC-DCC1 control technique	113
3.34	The DTC system using DTC-DCC2 control technique	114
4.1	The simulation results of torque, T_e , stator flux, φ_s , and stator currents, i_a , i_b and i_c , under matched DC voltages for (a) 1000 rpm (b) 600 rpm (c) 300 rpm	120
4.2	The experimental results of torque, T_e , stator flux, φ_s , and stator currents, i_a , i_b and i_c , under matched DC voltages for (a) 1000 rpm (b) 600 rpm (c) 300 rpm	121
4.3	The simulation results of stator flux sectors, d- and q- axis components of stator current and stator flux under matched DC voltages for (a) 1000 rpm (b) 600 rpm (c) 300 rpm	122
4.4	The experimental results of stator flux sectors, d- and q- axis components of stator current and stator flux under matched DC voltages for (a) 1000 rpm (b) 600 rpm (c) 300 rpm	123
4.5	The simulation results of stator current locus under matched DC voltages for (a) 1000 rpm (b) 600 rpm (c) 300 rpm	124
4.6	The experimental results of stator current locus under matched DC voltages for (a) 1000 rpm (b) 600 rpm (c) 300 rpm	124
4.7	The simulation results of stator flux locus under matched DC voltages for (a) 1000 rpm (b) 600 rpm (c) 300 rpm	125
4.8	The experimental results of stator flux locus under matched DC voltages for (a) 1000 rpm (b) 600 rpm (c) 300 rpm	125
4.9	The simulation results of torque, T_e , stator flux, φ_s , and stator currents, i_a , i_b and i_c , under mismatched DC voltages, $V_{dc1} = 100$ V, $V_{dc2} = 70$ V for (a) 1000 rpm (b) 600 rpm (c) 300 rpm	128
4.10	The experimental results of torque, T_e , stator flux, φ_s , and stator currents, i_a , i_b and i_c , under mismatched DC voltages, $V_{dc1} = 100$ V, $V_{dc2} = 70$ V for (a) 1000 rpm (b) 600 rpm (c) 300 rpm	129
4.11	The simulation results of stator flux sectors, d- and q- axis components of stator current and stator flux under mismatched DC voltages, $V_{dc1} = 100$ V, $V_{dc2} = 70$ V for (a) 1000 rpm (b) 600 rpm (c) 300 rpm	130

4.12	The experimental results of stator flux sectors, d- and q- axis components of stator current and stator flux under mismatched DC voltages, $V_{dc1} = 100$ V, $V_{dc2} = 70$ V for (a) 1000 rpm (b) 600 rpm (c) 300 rpm	131
4.13	The simulation results of d- and q- axis components of stator current locus using conventional sector under mismatched DC voltages, $V_{dc1} = 100$ V, $V_{dc2} = 70$ V for (a) 1000 rpm (b) 600 rpm (c) 300 rpm	133
4.14	The simulation results of d- and q- axis components of stator current locus using proposed sector under mismatched DC voltages, $V_{dc1} = 100$ V, $V_{dc2} = 70$ V for (a) 1000 rpm (b) 600 rpm (c) 300 rpm	133
4.15	The experimental results of d- and q- axis components of stator current locus using conventional sector under mismatched DC voltages, $V_{dc1} = 100$ V, $V_{dc2} = 70$ V for (a) 1000 rpm (b) 600 rpm (c) 300 rpm	133
4.16	The experimental results of d- and q- axis components of stator current locus using proposed sector under mismatched DC voltages, $V_{dc1} = 100$ V, $V_{dc2} = 70$ V for (a) 1000 rpm (b) 600 rpm (c) 300 rpm	134
4.17	The simulation results of stator flux locus using conventional sector under mismatched DC voltages, $V_{dc1} = 100$ V, $V_{dc2} = 70$ V for (a) 1000 rpm (b) 600 rpm (c) 300 rpm	134
4.18	The simulation results of stator flux locus using proposed sector under mismatched DC voltages, $V_{dc1} = 100$ V, $V_{dc2} = 70$ V for (a) 1000 rpm (b) 600 rpm (c) 300 rpm	135
4.19	The experimental results of stator flux locus using conventional sector under mismatched DC voltages, $V_{dc1} = 100$ V, $V_{dc2} = 70$ V for (a) 1000 rpm (b) 600 rpm (c) 300 rpm	135
4.20	The experimental results of stator flux locus using proposed sector under mismatched DC voltages, $V_{dc1} = 100$ V, $V_{dc2} = 70$ V for (a) 1000 rpm (b) 600 rpm (c) 300 rpm	135
4.21	The simulation results of torque, T_e , stator flux, φ_s , and stator currents, i_a , i_b and i_c , under mismatched DC voltages, $V_{dc1} = 100$ V, $V_{dc2} = 50$ V for (a) 1000 rpm (b) 600 rpm (c) 300 rpm	137

4.22	The experimental results of torque, T_e , stator flux, φ_s , and stator currents, i_a , i_b and i_c , under mismatched DC voltages, $V_{dc1} = 100$ V, $V_{dc2} = 50$ V for (a) 1000 rpm (b) 600 rpm (c) 300 rpm	138
4.23	The simulation results of stator flux sectors, d- and q- axis components of stator current and stator flux under mismatched DC voltages, $V_{dc1} = 100$ V, $V_{dc2} = 50$ V for (a) 1000 rpm (b) 600 rpm (c) 300 rpm	140
4.24	The experimental results of stator flux sectors, d- and q- axis components of stator current and stator flux under mismatched DC voltages, $V_{dc1} = 100$ V, $V_{dc2} = 50$ V for (a) 1000 rpm (b) 600 rpm (c) 300 rpm	141
4.25	The simulation results of d- and q- axis components of stator current locus using conventional sector under mismatched DC voltages, $V_{dc1} = 100$ V, $V_{dc2} = 50$ V for (a) 1000 rpm (b) 600 rpm (c) 300 rpm	142
4.26	The simulation results of d- and q- axis components of stator current locus using proposed sector under mismatched DC voltages, $V_{dc1} = 100$ V, $V_{dc2} = 50$ V for (a) 1000 rpm (b) 600 rpm (c) 300 rpm	143
4.27	The experimental results of d- and q- axis components of stator current locus using conventional sector under mismatched DC voltages, $V_{dc1} = 100$ V, $V_{dc2} = 50$ V for (a) 1000 rpm (b) 600 rpm (c) 300 rpm	144
4.28	The experimental results of d- and q- axis components of stator current locus using proposed sector under mismatched DC voltages, $V_{dc1} = 100$ V, $V_{dc2} = 50$ V for (a) 1000 rpm (b) 600 rpm (c) 300 rpm	144
4.29	The simulation results of d- and q- axis components of stator flux locus using conventional sector under mismatched DC voltages, $V_{dc1} = 100$ V, $V_{dc2} = 50$ V for (a) 1000 rpm (b) 600 rpm (c) 300 rpm	145
4.30	The simulation results of d- and q- axis components of stator flux locus using proposed sector under mismatched DC voltages, $V_{dc1} = 100$ V, $V_{dc2} = 50$ V for (a) 1000 rpm (b) 600 rpm (c) 300 rpm	145
4.31	The experimental results of d- and q- axis components of stator flux locus using conventional sector under mismatched DC	

	voltages, $V_{dc1} = 100$ V, $V_{dc2} = 50$ V for (a) 1000 rpm (b) 600 rpm (c) 300 rpm	146
4.32	The experimental results of d- and q- axis components of stator flux locus using proposed sector under mismatched DC voltages, $V_{dc1} = 100$ V, $V_{dc2} = 50$ V for (a) 1000 rpm (b) 600 rpm (c) 300 rpm	146
4.33	The simulation results of frequency spectrum and THD of stator current under matched DC voltages	147
4.34	The experimental results of frequency spectrum and THD of stator current under matched DC voltages	147
4.35	The simulation results of frequency spectrum and THD of stator current under mismatched DC voltages using conventional sector detector	148
4.36	The simulation results of frequency spectrum and THD of stator current under mismatched DC voltages using conventional sector detector	148
4.37	The experimental results of frequency spectrum and THD of stator current under mismatched DC voltages using conventional sector detector	149
4.38	The experimental results of frequency spectrum and THD of stator current under mismatched DC voltages using proposed sector detector	149
4.39	Torque, T_e and speed controls, ω under acceleration mode for matched DC voltages ratio 100:100 (a) simulation and (b) experiment results	152
4.40	Torque, T_e and speed controls, ω under deceleration mode for matched DC voltages ratio 100:100 (a) simulation and (b) experiment results	153
4.41	Simulation results of torque, T_e and speed controls, ω under acceleration mode for mismatched DC voltages ratio 100:70 for DTC OEWM with(a) conventional sector detector (b) proposed sector detector	154
4.42	Experimental results of torque, T_e and speed controls, ω under acceleration mode for mismatched DC voltages ratio 100:70 for DTC OEWM with(a) conventional sector detector (b) proposed sector detector	155

4.43	Simulation results of torque, T_e and speed controls, ω under deceleration mode for mismatched dc voltages ratio 100:70 for DTC OEWIM with (a) conventional sector detector (b) proposed sector detector	155
4.44	Experimental results of torque, T_e and speed controls, ω under deceleration mode for mismatched dc voltages ratio 100:70 for DTC OEWIM with (a) conventional sector detector (b) proposed sector detector	156
4.45	Simulation results of torque, T_e and speed controls, ω under acceleration mode for mismatched dc voltages ratio 100:50 for DTC OEWIM with (a) conventional sector detector (b) proposed sector detector	157
4.46	Experimental results of torque, T_e and speed controls, ω under acceleration mode for mismatched dc voltages ratio 100:50 for DTC OEWIM with (a) conventional sector detector (b) proposed sector detector	157
4.47	Simulation results of torque, T_e and speed controls, ω under deceleration mode for mismatched dc voltages ratio 100:50 for DTC OEWIM with (a) conventional sector detector (b) proposed sector detector	158
4.48	Experimental results of torque, T_e and speed controls, ω under deceleration mode for mismatched dc voltages ratio 100:50 for DTC OEWIM with (a) conventional sector detector (b) proposed sector detector	158
4.49	Simulation result of Torque, T_e and Phase Voltage, V_{an} under DTC-LVV and DTC-SVV (a) Full scale (b) Magnified version	161
4.50	Experimental result of Torque, T_e and Phase Voltage, V_{an} under DTC-LVV and DTC-SVV (a) Full scale (b) Magnified version	161
4.51	Simulation result of Torque, T_e and Phase Voltage, V_{an} under DTC-SVV and DTC-DCC1 (a) Full scale (b) Magnified version	163
4.52	Experimental result of Torque, T_e and Phase Voltage, V_{an} under DTC-SVV and DTC-DCC1 (a) Full scale (b) Magnified version	163
4.53	Simulation result of Torque, T_e and Phase Voltage, V_{an} under DTC-SVV and DTC-DCC2 (a) Full scale (b) Magnified version	164
4.54	Experimental result of Torque, T_e and Phase Voltage, V_{an} under DTC-SVV and DTC-DCC2 (a) Full scale (b) Magnified version	165

4.55	Simulation result of Torque, T_e and Phase Voltage, V_{an} under DTC-SVV and DTC-DCC2 using 0.25Nm hysteresis band (a) Full scale (b) Magnified version	166
4.56	Experimental result of Torque, T_e and Phase Voltage, V_{an} under DTC-SVV and DTC-DCC2 using 0.25Nm hysteresis band (a) Full scale (b) Magnified version	167
4.57	Simulation results of stator current, i_a and FFT spectrum for (a) Stator current of DTC-LVV and (b) FFT of DTC-LVV	169
4.58	Experimental results of stator current, i_a and FFT spectrum for (a) Current of DTC-LVV and (b) FFT of DTC-LVV	170
4.59	Simulation results of stator current, i_a and FFT spectrum for (a) Current of DTC-SVV and (b) FFT of DTC-SVV	171
4.60	Experimental results of stator current, i_a and FFT spectrum for (a) Current of DTC-SVV and (b) FFT of DTC-SVV	171
4.61	Simulation results of stator current, i_a and FFT spectrum for (a) Current of DTC-DCC1 and (b) FFT of DTC-DCC1	172
4.62	Experimental results of stator current, i_a and FFT spectrum for (a) Current of DTC-DCC1 and (b) FFT of DTC-DCC1	173
4.63	Simulation results of stator current, i_a and FFT spectrum for (a) Current of DTC-DCC2 and (b) FFT of DTC-DCC2	174
4.64	Experimental results of stator current, i_a and FFT spectrum for (a) Current of DTC-DCC2 and (b) FFT of DTC-DCC2	174
4.65	Simulation results of dynamic operation of torque by using DTC-LVV	177
4.66	Magnified view of simulation results for dynamic torque operation using DTC-LVV	177
4.67	Experimental results of dynamic operation of torque by using DTC-LVV	177
4.68	Magnified view of experimental results for dynamic torque operation using DTC-LVV	178
4.69	Simulation results of dynamic operation of torque by using DTC-SVV	179

4.70	Magnified view of simulation results for dynamic torque operation using DTC-SVV	179
4.71	Experimental results of dynamic operation of torque by using DTC-SVV	179
4.72	Magnified view of experimental results for dynamic torque operation using DTC-SVV	180
4.73	Simulation results of dynamic operation of torque by using DTC-DCC1	181
4.74	Magnified view of simulation results for dynamic torque operation using DTC-DCC1	181
4.75	Experimental results of dynamic operation of torque by using DTC-DCC1	181
4.76	Magnified view of experimental results for dynamic torque operation using DTC-DCC1	182
4.77	Simulation results of dynamic operation of torque by using DTC-DCC2	183
4.78	Magnified view of simulation results for dynamic torque operation using DTC-DCC2	183
4.79	Experimental results of dynamic operation of torque by using DTC-DCC2	183
4.80	Magnified view of experimental results for dynamic torque operation using DTC-DCC2	184

LIST OF APPENDICES

APPENDIX	TITLE	PAGE
A	C-code language programming of look-up table	209
B	C-code language programming of flux sector	217
C	Simulation Model of the Conventional DTC-OEWIM	218
D	Lab Scale Experimental Arrangements	224
E	Datasheet of IGBT	232

